



**Journal of  
Mechanics of  
Materials and Structures**

**FRACTURE IN THREE DIMENSIONS DUE TO DIE MOTION ON  
CRACK SURFACES: FRAMEWORK FOR STUDY OF  
CRACK/CONTACT ZONE GEOMETRY**

Louis M. Brock

**Volume 12, No. 2**

**March 2017**





## **FRACTURE IN THREE DIMENSIONS DUE TO DIE MOTION ON CRACK SURFACES: FRAMEWORK FOR STUDY OF CRACK/CONTACT ZONE GEOMETRY**

LOUIS M. BROCK

Dynamic steady state growth in 3D of a semi-infinite plane crack in isotropic elastic solids is considered. Growth is driven by the translation of a rigid die between the two crack surfaces. Sliding friction is neglected, but the possibility that crack surfaces resume contact in the wake of the die is considered. Translation and crack growth occur at the same, constant, subcritical speed. An analytical solution is obtained, and a criterion for fracture based on dynamic energy release rate imposed, with kinetic energy included. A nonlinear differential equation for crack edge location and constraint equations result, and together form a framework for study of crack and contact zone geometry.

### **Introduction**

One result of 2D studies of dynamic fracture is an equation of motion for the crack tip [Freund 1990]. In a 3D study, such an equation must describe the contour defined by the crack edge in the crack plane. For the dynamic steady state, this goal is considered in [Brock 2015a] for semi-infinite crack growth in an unbounded solid. [Brock 2015b] extends this effort in two ways:

- (a) Per the standard model [Freund 1990], dynamic energy release rate is equated with surface energy.
- (b) The standard model is itself modified by the inclusion of kinetic energy [Gdoutos 2005].

As in [Brock 2015a], the crack remains in its original plane, and growth is caused by translation at constant subcritical speed of compression loads on the crack faces. Such growth can be viewed as an example of hydraulic fracture, e.g., [Mastrojannis et al. 1980]. The present article considers fracture driven not by specified crack face loading, but by wedging, i.e., rigid die motion between faces of an initially closed crack.

The 2D, dynamic steady state study of sliding contact, e.g., [Brock and Georgiadis 2000], shows that for subcritical sliding speed the apex of a smooth-contoured, convex rigid die lies within the contact zone. In subsequent 2D studies, e.g., [Brock 2004], semi-infinite crack extension by the wedging action of such a die exhibits the same behavior. Moreover, crack closure (crack surfaces resuming contact in the wake of the die) is possible. This paper considers the same possibility.

The problem statement and governing equations begin the analysis. The unmixed problem for (largely unspecified) discontinuities in displacement and traction over a planar area in the same solid is then addressed. Integral transforms are obtained, and analytical expressions for the inverses applied to the fracture problem. As stated above, sliding contact is frictionless. For purposes of illustration and possible application in future work, however, this part of the analysis incorporates sliding friction. A framework

---

*Keywords:* 3D, dynamic, criteria, contact zone, crack edge, kinetic energy.

of equations is developed and its application in the frictionless limit allows study of both crack and contact zone contours.

### Problem statement and governing equations

An unbounded isotropic solid is at rest, but contains a closed slit. In Cartesian basis  $\mathbf{x} = \mathbf{x}(x_k)$ ,  $k = (1, 2, 3)$  the slit comprises semi-infinite region ( $x_3 = 0, x_1 < 0$ ) with boundary  $B_S$  ( $x_1 = 0$ ). A rigid die is inserted in the slit, and its shape and placement guarantee symmetry with respect to both the  $x_1x_2$ -plane and  $x_2x_3$ -plane. The die then translates in the positive  $x_1$ -direction at subcritical constant speed  $V$ . Translation is opposed by friction, and contact zone  $A_C$  with closed boundary  $B_C$  forms on each slit face. Fracture occurs so that  $B_S$  also moves, and may no longer be rectilinear. Crack closure, i.e., surfaces resume contact [Brock 2004], is allowed in the wake of the die. Thus a crack gap exists in region  $A_G$  between  $B_S$  and a contour  $B_C^-$ , and  $A_C \in A_G$ . The crack closure region is designated  $A_C^-$ , and the nonfractured region ahead of  $B_S$  is designated as  $A_N$ . Contour  $B_C^-$  is also of infinite length, and not necessarily rectilinear. A dynamic steady state ensues, such that  $(B_S, B_C, B_C^-)$  no longer change shape but translate in the positive  $x_1$ -direction with speed  $V$ . Displacement  $\mathbf{u}(u_k)$  and traction  $\mathbf{T}(\sigma_{ik})$  do not vary in the moving frame of  $(B_S, B_C, B_C^-)$ . Basis  $\mathbf{x}$  is therefore also translated with speed  $V$  so that  $u_k = u_k(\mathbf{x})$ ,  $\sigma_{ik} = \sigma_{ik}(\mathbf{x})$  and the (absolute) time derivative  $(Df, \dot{f})$  can be written  $-V\partial_1 f$ . Here  $\partial_k f$  signifies  $x_k$ -differentiation. For convenience, the origin of  $\mathbf{x}$  is placed in  $A_C$ . Die shape and expectations that  $(B_S, B_C, B_C^-)$  do not intersect suggest that contours and contour gradients can be defined by single-valued, continuous functions of  $(x_1, x_2)$ .

The equations that govern  $(\mathbf{u}, \mathbf{T})$  in the unbounded solid are [Brock 2015a; 2015b]:

$$\nabla \cdot \mathbf{T} - \rho V^2 \partial_1^2 \mathbf{u} = 0, \quad (1a)$$

$$\frac{1}{\mu} \mathbf{T} = \frac{2\nu}{1-2\nu} (\nabla \cdot \mathbf{u}) \mathbf{1} + \nabla \mathbf{u} + \mathbf{u} \nabla. \quad (1b)$$

In (1)  $(\nabla, \nabla^2, \mathbf{1})$  respectively are gradient, Laplacian, and identity tensor. Constant  $(\mu, \rho, \nu)$  are shear modulus, mass density and Poisson's ratio. Equation (1) embodies the assumption that body forces can be neglected, and uncoupling gives

$$\mathbf{u} = \mathbf{u}_S + \mathbf{u}_D, \quad (2a)$$

$$(\nabla^2 - c^2 \partial_1^2) \mathbf{u}_S = 0, \quad (c_D^2 \nabla^2 - c^2 \partial_1^2) \mathbf{u}_D = 0, \quad (2b)$$

$$\nabla \cdot \mathbf{u}_S = 0, \quad \nabla \times \mathbf{u}_D = 0. \quad (2c)$$

Dimensionless quantities are also introduced as

$$c = V/V_S, \quad c_D = V_D/V_S = \sqrt{m+1}, \quad m = 1/(1-2\nu). \quad (3a)$$

Here  $(V_S, V_D)$  are shear and dilatational wave speeds, and

$$V_S = \sqrt{\mu/\rho}. \quad (3b)$$

Conditions for  $x_3 = 0, (x_1, x_2) \in (A_N, A_C^-)$  are

$$[u_k] = [\sigma_{3k}] = 0. \quad (4a)$$

Here  $[f] = f^{(+)} - f^{(-)}$  and  $f^{(\pm)}$  signifies evaluation at  $x_3 = 0(\pm)$ . Equation (4a) therefore embodies the assumption that slip does not occur in slit closure region  $A_C^-$ . Singular behavior of  $(\mathbf{T}, \nabla \mathbf{u})$  is expected near  $B_S$ , but not near  $(B_C, B_C^-)$ . In  $A_G - A_C$

$$[\sigma_{3k}] = \sigma_{3k}^{(\pm)} = 0. \quad (4b)$$

Mixed conditions (for infinitesimal deformation) hold in  $A_C$  as

$$\mathbf{u}_3^{(\pm)} = (\mp)U, \quad [u_1] = [u_2] = 0, \quad (4c)$$

$$\sigma_{31}^{(\pm)} = (\pm)\gamma\sigma_{33}^{(\pm)}, \quad \sigma_{32}^{(\pm)} = 0, \quad [\sigma_{33}] = 0. \quad (4d)$$

Here  $\gamma$  is the (dimensionless) friction coefficient. Function  $U(x_1, x_2)$  is defined by shape and orientation of the die, and thus is bounded, continuous and symmetric in  $x_2$ . The inhomogeneous Equation (4c) involves bounded terms, and (4c) and (4d) hold in finite region  $A_C$ . Solutions  $(\mathbf{u}, \mathbf{T})$  should therefore be finite for  $|\mathbf{x}| \rightarrow \infty$ .

Constraints also apply:

- (I) Traction in  $A_C$  is finite and continuous.
- (II) Normal traction is nontensile in  $(A_C, A_C^-)$  and tensile near  $B_C$  in  $A_N$ .
- (III) Normal traction in  $A_C$  is invariant with respect to resultant compressive force on  $A_C$  [Brock 2012].
- (IV) The dynamic energy release rate criterion [Freund 1972] governs, with kinetic energy included [Gdoutos 2005; Brock 2015b].

### Related problem: translating discontinuities

As in [Brock 2015a; 2015b], an unmixed problem for translation of discontinuities in displacement and traction on the  $x_1x_2$ -plane is considered first. Equations (1)–(3) again hold, and the solution is also bounded for  $|\mathbf{x}| \rightarrow \infty$ .  $([u_k], [\sigma_{3k}])$  vanish for  $(x_1, x_2) \notin A_G$ , and are piecewise continuous functions of  $(x_1, x_2) \in A_G$ . Equations (4c) and (4d) are therefore replaced by

$$[u_k] = [\sigma_{3k}] = 0 \quad (x_1, x_2) \notin A_G. \quad (5)$$

For  $(x_1, x_2) \in A_G$  components of  $[\mathbf{u}]$  are bounded, but near  $B_C$  components of  $[\sigma_{3k}]$  can be singular. The double bilateral transform [Sneddon 1972] is now introduced as

$$\hat{f} = \iint_{12} f(x_1, x_2) \exp(-p_1x_1 - p_2x_2) dx_1 dx_2. \quad (6)$$

Symbol 12 signifies integration over the  $x_1x_2$ -plane. Application of (6) to (1)–(3) gives

$$\hat{\mathbf{u}}_S = \mathbf{V}^{(\pm)} \exp(-B|x_3|), \quad \hat{\mathbf{u}}_D = \mathbf{U}_D^{(\pm)} \exp(-A|x_3|). \quad (7)$$

Superscript  $(\pm)$  signifies  $x_3 \geq 0$  and  $x_3 \leq 0$ , respectively, and

$$p_1 V_1^{(\pm)} + p_2 V_2^{(\pm)} (\mp) B V_3^{(\pm)} = 0, \quad (8a)$$

$$(U_D)_1^{(\pm)} = p_1 U_D^{(\pm)}, \quad (U_D)_2^{(\pm)} = p_2 U_D^{(\pm)}, \quad (U_D)_3^{(\pm)} = (\mp) A_{\pm} U_D^{(\pm)}, \quad (8b)$$

$$B = \sqrt{c_1^2 - p_1^2 - p_2^2}, \quad A = \sqrt{c_1^2/c_D^2 - p_1^2 - p_2^2}, \quad c_1 = c p_1. \quad (8c)$$

Here  $(V_1^{(\pm)}, V_2^{(\pm)}, U_D^{(\pm)})$  are arbitrary functions of  $(p_1, p_2)$ , and bounded behavior of (7) as  $|x_3| \rightarrow \infty$  requires that  $\text{Re}(B, A) \geq 0$  in the cut  $(p_1, p_2)$ -planes. Use of (5)–(8) gives six equations for finding  $(V_1^{(\pm)}, V_2^{(\pm)}, U^{(\pm)})$  in terms of  $([\hat{u}_k], [\hat{\sigma}_{3k}])$ . Solutions are given in Appendix A by (A.1) and (A.2). Together with the transform of (1b) they generate (A.3).

### Transform inversion — general formulas

Equations (4c) and (4d) indicate that application of related problem results to the crack growth problem requires expressions that relate  $([u_k], [\sigma_{3k}], \sigma_{3k}^{(+)})$ . Therefore (A.3) is subjected to the inversion operation corresponding to (6). This results in three equations of the general form

$$\sum_j \iint_G f_j d\xi_1 d\xi_2 \left(\frac{1}{2\pi i}\right)^2 \iint dp_1 dp_2 C_j \exp[p_1(x_1 - \xi_1) + p_2(x_2 - \xi_2)] = 0. \quad (9)$$

Here  $f_j(\xi_1, \xi_2)$  represents  $([u_k], [\sigma_{3k}], \sigma_{3k}^{(+)})$  and  $C_j(p_1, p_2)$ , coefficient of the corresponding transform in (A.3). Subscript  $G$  signifies integration over  $A_G$ , and the remaining integrals are taken over the entire  $\text{Im}(p_1)$ - and  $\text{Im}(p_2)$ -axes. Results in [Brock 2012; 2015a; 2015b] suggest use of transformations

$$p_1 = p \cos \psi, \quad p_2 = p \sin \psi, \quad (10a)$$

$$\begin{bmatrix} x \\ y \end{bmatrix} = \begin{bmatrix} \cos \psi & \sin \psi \\ -\sin \psi & \cos \psi \end{bmatrix} \begin{bmatrix} x_1 \\ x_2 \end{bmatrix}, \quad \begin{bmatrix} \xi \\ \eta \end{bmatrix} = \begin{bmatrix} \cos \psi & \sin \psi \\ -\sin \psi & \cos \psi \end{bmatrix} \begin{bmatrix} \xi_1 \\ \xi_2 \end{bmatrix}. \quad (10b)$$

Here  $\text{Re}(p) = 0+$ ,  $|\text{Im}(p), x, y, \xi, \eta| < \infty$  and  $|\psi| < \pi/2$ . Parameters  $(p, \psi)$ ,  $(x, \psi; y = 0)$  and  $(\xi, \psi; \eta = 0)$  resemble quasipolar coordinates, i.e.,

$$dx_1 dx_2 = |x| dx d\psi, \quad d\xi_1 d\xi_2 = |\xi| d\xi d\psi, \quad dp_1 dp_2 = |p| dp d\psi. \quad (10c)$$

In (8) and (A.1)–(A.3), quantities  $(A, B, T, D_R, D_N, D_M)$  can be written as products of functions of  $p$  and, respectively, factors as

$$A = \sqrt{1 - \bar{c}^2/c_D^2}, \quad B = \sqrt{1 - \bar{c}^2}, \quad T = \bar{c}^2 - 2, \quad (11a)$$

$$R = 4AB - T^2, \quad N = 2AB + T, \quad M = 2N + \bar{c}^2 \quad (11b)$$

$$\bar{c} = c \cos \psi. \quad (11c)$$

For  $\text{Re}(A, B) \geq 0$  the requirement that  $\text{Re}(\sqrt{\pm p}) > 0$  respectively, in the cut  $p$ -plane with branches  $\text{Im}(p) = 0, \text{Re}(p) < 0$  and  $\text{Im}(p) = 0, \text{Re}(p) > 0$  guarantees that (7) is bounded. However  $\text{Re}(A, B) \geq 0$

requires  $0 < c < 1$ , i.e., translation speed is restricted to range  $0 < V < V_S$ . Equation (9) assumes the general form

$$\sum_j \frac{1}{i\pi} \int_{\Psi} C_j d\psi \int_{G\eta} d\eta \int_{G\xi} f_j d\xi \frac{1}{2\pi i} \int \frac{|p|}{p} dp \left( 1, \frac{\sqrt{-p}}{\sqrt{p}} \right) \exp p(x - \xi) = 0. \quad (12a)$$

Now  $f_j = f_j(x, \psi; \eta)$  represents  $(\partial[u_k]/\partial\xi, [\sigma_{3k}], \sigma_{3k}^{(+)})$  and  $C_j = C_j(\psi)$ . Integration is along the positive side ( $\text{Re}(p) = 0+$ ) of the entire  $\text{Im}(p)$ -axis, and  $p$ -dependence is seen to be of two types. Symbol  $\Psi$  signifies integration over range  $|\psi| < \pi/2$ . Symbols ( $G\xi, G\eta$ ) signify integration with respect to  $(\xi, \eta)$  over  $A_G$ . Performance of the  $p$ -integration [Brock 2015a; 2015b] gives

$$\sum_j \int_{\Psi} C_j d\psi \int_{G\eta} d\eta \left( f_j, \frac{1}{\pi} \int_{G\xi} \frac{f_j d\xi}{\xi - x} \right) = 0. \quad (12b)$$

The first (nonintegral) term in parentheses vanishes for  $x \notin G\xi$  and appears for  $x \in G\xi$ ; the integral (second term) is then evaluated in the principal value ( $vp$ ) sense. It is noted that  $(A_G, A_C, A_{\bar{C}}, A_N)$  and  $(\partial[u_k]/\partial\xi, [\sigma_{3k}], \sigma_{3k}^{(+)})$  can be defined completely in terms of  $(x, \psi)$ , and that

$$f(x, \psi) = -\frac{\partial}{\partial x} \int_{G\eta} d\eta \int_{G\xi} d\xi f(\xi, \psi) \delta(x - \xi) \delta(\eta). \quad (12c)$$

Here  $\delta$  is the Dirac function. These results imply that form (12b) is satisfied when

$$\sum C_j(\psi) \left[ f_j(x, \psi), \frac{1}{\pi} \int_{G\xi} f_j(\xi, \psi) \frac{d\xi}{\xi - x} \right] = 0.$$

In light of this equality, together with (10)–(12) and (A.3), the three equations in (A.3) give for  $x_3 = 0(+)$ ,  $|\psi| < \pi/2$ :

$$\frac{\partial}{\partial x} [u_1] = \frac{\cos \psi}{\mu R} [\sigma_{33}] + \frac{2}{\mu R \pi} \int_{GX} \frac{d\xi}{\xi - x} [g_{12}(\sigma_{32}^{(+)} - [\sigma_{32}]/2) + g_{11}(\sigma_{31}^{(+)} - [\sigma_{31}]/2)], \quad (13a)$$

$$\frac{\partial}{\partial x} [u_2] = \frac{\sin \psi}{\mu R} [\sigma_{33}] + \frac{2}{\mu R \pi} \int_{GX} \frac{d\xi}{\xi - x} [g_{21}(\sigma_{31}^{(+)} - [\sigma_{31}]/2) + g_{22}(\sigma_{32}^{(+)} - [\sigma_{32}]/2)], \quad (13b)$$

$$\frac{\partial}{\partial x} [u_3] = \frac{N}{\mu R} [[\sigma_{31}] \cos \psi + [\sigma_{32}] \sin \psi] - \frac{2\bar{c}^2 A}{\mu R \pi} \int_{GX} \frac{d\xi}{\xi - x} (\sigma_{33}^{(+)} - [\sigma_{33}]/2), \quad (13c)$$

$$g_1 = M/B \sin^2 \psi + \bar{c}^2 B, \quad g_2 = M/B \cos^2 \psi + \bar{c}^2 B, \quad g_{12} = -M/B \sin \psi \cos \psi. \quad (13d)$$

Subscript  $GX$  signifies integration over those segments of  $G\xi$  in which integrand terms do not vanish. In (11) and (13),  $R$  is the Rayleigh function, where  $R \rightarrow 0+$  ( $\bar{c} = 0$ ),  $R = -1$  ( $\bar{c} = 1$ ) and  $R = 0$  ( $\bar{c} = c_R$ ,  $0 < c_R < 1$ ). Term  $\bar{c} < c$  for  $|\psi| < \pi/2$  in (11c), so that restriction  $0 < V < V_R$  now applies, where  $V_R = c_R V_S$  is the Rayleigh speed.

### Basic solution to crack growth problem

In view of (5), (10) and conditions (4) imposed on  $(A_G, A_C)$  and  $(B_S, B_C, B_C^-)$ , the geometry of these regions on  $x_3 = 0$  can be defined for  $|\psi| < \pi/2$  as

$$A_C : -r_-(\psi) < x < r_+(\psi), \quad (14a)$$

$$A_G : -r_C^-(\psi) < x < r_S(\psi), \quad (14b)$$

$$A_G - A_C : -r_C^-(\psi) < x < -r_-(\psi), \quad r_+(\psi) < x < r_S(\psi), \quad (14c)$$

$$A_C^- : x < -r_C^-(\psi), \quad A_N : x > r_C(\psi). \quad (14d)$$

Here  $(r_\pm, r_S, r_C^-) > 0$ , and a continuous boundary  $B_C$  requires that  $r_+(\pm\pi/2) = r_-(\mp\pi/2)$ . In view of, e.g., [Brock 2004], it is reasonable to expect that  $(r_S, r_C^-) \gg r_\pm$ , but this expectation plays no role until the basic solution is illustrated for a specific die geometry. Equations (4) and (10) indicate that for  $x_3 = 0(+)$ ,  $|\psi| < \pi/2$

$$A_C : [\sigma_{32}] = [\sigma_{33}] = \sigma_{32}^{(+)} = 0, \quad \frac{\partial}{\partial x}[u_1] = \frac{\partial}{\partial x}[u_2] = 0, \quad (15a)$$

$$A_G - A_C : [\sigma_{3k}] = \sigma_{3k}^{(+)} = 0, \quad k = (1, 2, 3), \quad (15b)$$

$$(A_C^-, A_N) : [\sigma_{3k}] = \frac{\partial}{\partial x}[u_k] = 0, \quad k = (1, 2, 3). \quad (15c)$$

In addition, properties assumed for the die suggest that

$$A_N : \sigma_{31}^{(+)} = \sigma_{32}^{(+)} = 0, \quad (16a)$$

$$A_C : [u_3] = 2u_3^{(+)}, \quad [\sigma_{31}] = 2\sigma_{31}^{(+)}. \quad (16b)$$

Equations (13a) and (13b) are thus satisfied when  $([u_1], [u_2]) \equiv 0$ . Notation  $(\sigma_{33}^{(\pm)} \rightarrow \sigma, \xi \rightarrow t)$  is introduced in (13c), which in view of (4c) and (10) gives

$$A_C^- : (vp) \int_{C-} \frac{\sigma dt}{t-x} + \int_C \frac{\sigma dt}{t-x} + \int_N \frac{\sigma dt}{t-x} = 0, \quad (17a)$$

$$A_0 : -\frac{2\bar{c}^2 A}{\mu R \pi} \left[ \int_{C-} \frac{\sigma dt}{t-x} + (vp) \int_C \frac{\sigma dt}{t-x} + \int_N \frac{\sigma dt}{t-x} \right] + \frac{2N}{\mu R} \gamma \sigma \cos \psi = -2 \frac{\partial U}{\partial x}, \quad (17b)$$

$$A_N : \int_{C-} \frac{\sigma dt}{t-x} + \int_C \frac{\sigma dt}{t-x} + (vp) \int_N \frac{\sigma dt}{t-x} = 0. \quad (17c)$$

Subscripts  $(C-, C, N)$  respectively signify integration over range  $t < -r_C^-$ ,  $-r_- < t < r_+$  and  $t > r_S$ . Solution of set (17) for  $(x, \psi) \in A_C$  and  $(x, \psi) \in (A_C^-, A_N)$  respectively, is

$$\frac{\sigma}{\mu} = \frac{R}{S} \left[ \frac{\partial U}{\partial x} \cos \pi \Omega + \sin \pi \Omega \sqrt{\frac{x+r_C^-}{r_S-x}} \frac{(r_+-x)^{1+\Omega}}{(x+r_-)^\Omega} (vp) Q_C \left( \frac{\partial U}{\partial x}; x \right) \right], \quad (18a)$$



$$\frac{\sigma}{\mu} = \frac{R}{S} \sqrt{\frac{x+r_C^-}{x-r_S} \frac{(x-r_+)^{1+\Omega}}{(x+r_-)^\Omega}} Q_C\left(\frac{\partial U}{\partial x}; x\right), \quad (18b)$$

$$Q_C(f; \xi) = \frac{1}{\pi} \int_C f \sqrt{\frac{r_S-t}{t+r_C^-} \frac{(t+r_-)^\Omega}{(r_+-t)^{1+\Omega}}} \frac{dt}{t-\xi}. \quad (18c)$$

Equation (18a) satisfies constraint I when

$$\int_C \frac{\partial U}{\partial t} \sqrt{\frac{r_S-t}{t+r_C^-} \frac{(t+r_-)^\Omega}{(r_+-t)^{1+\Omega}}} \frac{dt}{t-r_+} = 0. \quad (18d)$$

In (18a) and (18b) terms  $(\Omega, S)$  are defined as

$$\Omega = -\frac{1}{2} + \Gamma < 0, \quad \Gamma = \frac{1}{\pi} \tan^{-1} \left( \frac{-\gamma N \cos \psi}{\bar{c}^2 A} \right) > 0, \quad (19a)$$

$$S = \sqrt{(\gamma N \cos \psi)^2 + (\bar{c}^2 A)^2}. \quad (19b)$$

For  $r_+ < x < r_S$  and  $-r_C^- < x < -r_-$  respectively in  $A_G - A_C$

$$\frac{\partial}{\partial x} [u_3] = \frac{2\bar{c}^2 A}{S} \sqrt{\frac{x+r_C^-}{r_S-x} \frac{(x-r_+)^{1+\Omega}}{(x+r_-)^\Omega}} Q_C\left(\frac{\partial U}{\partial x}; x\right), \quad (20a)$$

$$\frac{\partial}{\partial x} [u_3] = -\frac{2\bar{c}^2 A}{S} \sqrt{\frac{x+r_C^-}{r_S-x} \frac{(r_+-x)^{1+\Omega}}{(-x-r_-)^\Omega}} Q_C\left(\frac{\partial U}{\partial x}; x\right). \quad (20b)$$

Knowledge of  $([u_3], \partial_1[u_3])$  for  $r_+ < x < r_S$  will be required. Equations (10) and (20a) provide ingredients for this with

$$[u_3] = -\frac{2\bar{c}^2 A}{S\pi} \int_C \frac{\partial U}{\partial t} dt \sqrt{\frac{r_S-t}{t+r_C^-} \frac{(t+r_-)^\Omega}{(r_+-t)^{1+\Omega}}} \int_+ \sqrt{\frac{\tau+r_C^-}{r_S-\tau} \frac{(\tau-r_+)^{1+\Omega}}{(\tau+r_-)^\Omega}} \frac{d\tau}{\tau-t}, \quad (21a)$$

$$\partial_1 f = \cos \psi \frac{\partial f}{\partial x} - \frac{\sin \psi}{|x|} \frac{\partial f}{\partial \psi}, \quad \partial_2 f = \sin \psi \frac{\partial f}{\partial x} + \frac{\cos \psi}{|x|} \frac{\partial f}{\partial \psi}. \quad (21b)$$

Symbol  $\int_+$  signifies integration over range  $x < \tau < r_S$ . As is appropriate, (21a) vanishes for  $x \rightarrow r_S^-$ .

### Constraint (I, II, III): preliminary observations

Contour parameters  $r_\pm(\psi)$ ,  $r_S(\psi)$  and  $r_C^-(\psi)$  remain to be determined. Equation (18d) provides one equation, and (18a) must satisfy (unilateral) constraint II. If such is indeed the case, the resultant force on each contact zone  $A_C$  is

$$-\int_\Psi d\psi \int_C |x| \sigma(x, \psi) dx. \quad (22a)$$

Constraint III requires that  $\sigma$  be invariant with respect to the force, i.e., for arbitrary  $(\delta x, \delta \psi)$

$$\delta \sigma = \frac{\partial \sigma}{\partial x} \delta x + \frac{\partial \sigma}{\partial \psi} \delta \psi = 0. \quad (22b)$$

Therefore for  $-r_- < x^* < r_+$

$$\frac{\partial \sigma}{\partial x}(x^*, \psi) = 0, \quad \frac{\partial \sigma}{\partial \psi}(x^*, \psi) = 0. \quad (22c)$$

Equation (22) is examined below in terms of specific die geometry ( $U$ ).

#### Constraint IV: dynamic energy release rate

In this study kinetic energy is considered [Brock 2015b; Gdoutos 2005]. Nevertheless known procedures, e.g., [Freund 1972], can be used to derive the balance equation required by constraint IV:

$$D \iint_G e_G dx_1 dx_2 = \iint_0 [\sigma_{3k} \dot{u}_k] dx_1 dx_2 + D \iiint_{123} \frac{\rho}{2} \dot{u}_k \dot{u}_k dx_1 dx_2 dx_3. \quad (23)$$

Subscript 123 signifies integration over the unbounded solid. Subscript 0, integration over a thin strip that straddles crack edge  $B_S$  and subscript  $G$ , integration over gap surface  $A_G$ . Term  $e_G$  is the surface energy per unit area of  $A_G$ , and is treated as constant [deBoer et al. 1988; Skriver and Rosengard 1992; Freund 1990]. The presence of operators ( $\dot{f}$ ,  $Df$ ) signifies fixed basis  $\mathbf{x}$ . Use of translating basis  $\mathbf{x}$  and Green's theorem [Malvern 1969], imposition of the dynamic steady state, and use of (10) give for the first term in (23),

$$V e_G \int_{\psi} \sqrt{r_S^2 + (r_S')^2} \cos \psi d\psi. \quad (24a)$$

Here  $f'$  signifies  $df/d\psi$  and it is noted that the radical in (24a) can be written as

$$r_S \sqrt{D_S^2 + D_C^2}, \quad (24b)$$

with

$$D_S = \frac{1}{r_S} (r_S \sin \psi)', \quad D_C = \frac{1}{r_S} (r_S \cos \psi)'. \quad (24c)$$

Because  $([u_1], [u_2]) \equiv 0$ , use of (10) gives for the second integral in (23),

$$\mu V \int_{\psi} d\psi \int_{-}^{+} |x| dx \sigma \partial_1 [u_3]. \quad (25)$$

Here  $\pm$  signifies integration limits  $r_S \pm$ . Term  $(\sigma, [u_3]) = 0$  for  $r_+ < x < r_S$  and  $x > r_S$ , respectively. In view of (18b) and (20a), however:

$$\frac{\sigma}{\mu} \approx \frac{R}{S} \frac{G_C}{\pi \sqrt{x - r_S}} (x \rightarrow r_S+), \quad (26a)$$

$$\frac{\partial}{\partial x} [u_3] \approx -\frac{2\bar{c}^2 A}{S} \frac{G_C}{\pi \sqrt{r_S - x}} (x \rightarrow r_S-), \quad (26b)$$

$$G_C = \sqrt{l_G} \frac{(r_S - r_+)^{1+\Omega}}{(r_S + r_-)^{\Omega}} \int_C \frac{\partial U}{\partial t} \frac{(t + r_-)^{\Omega}}{(r_+ - t)^{1+\Omega}} \frac{dt}{\sqrt{t + r_C^-} \sqrt{r_S - t}}, \quad l_G = r_S + r_C^-. \quad (26c)$$

Equation (26a) must give positive  $\sigma$  (constraint II), and this requires that  $G_C > 0$ . Distance between  $B_S$  and  $B_C^-$ , measured along a line passing through  $(x_1, x_2) = 0$ , is  $l_G$ . In view of (21b),  $\partial_1 [u_3]$  exhibits (26b), but also the derivative of (21a) with respect to  $\psi$ . Chain/product-rule differentiation is required for

this. Quantity  $U$  and parameters involving  $(\Omega, \bar{c})$  are given functions of  $\psi$ , but  $(r_{\pm}, r_S, r_C^-)$  are not. For  $x \rightarrow r_S^-$  however, the dominant contribution involves  $r'_S$ , and  $\partial[u_3]/\partial r_S = -\partial[u_3]/\partial x$ . Equation (21b) then gives

$$\partial_1[u_3] \approx -\frac{2\bar{c}^2 A}{S} \frac{G_C D_S}{\pi \sqrt{r_S - x}} \quad (x \rightarrow r_S^-). \quad (27a)$$

In view of (26a) and (27a) the  $x$ -integrand exhibits Dirac function  $\delta(x - r_S)$  [Freund 1972], so that (25) gives

$$\frac{\mu V}{2\pi} \int_{\Psi} d\psi \frac{R}{S} G_C^2 r_S D_S. \quad (27b)$$

Singular behavior as  $x \rightarrow r_S$  and rapid decay as  $|x| \rightarrow \infty$  seen in (26) are manifest in  $\nabla \mathbf{u}$  generally. Therefore integration in the third term in (23) can be confined to a tube of radius  $r_B \rightarrow 0$  that encloses  $B_S$ . Term  $\dot{u}_k = -V \partial_1 u_k$  in translating basis  $\mathbf{x}$  for the dynamic steady state, and 3D expressions for  $\sqrt{(x - r_S)^2 + x_3^2} < r_B$ ,  $|\psi| < \pi/2$  are required. Equations (A.1) and (7) lead to  $\hat{\mathbf{u}}(p_1, p_2, x_3)$ , and relevant components are given in Appendix B. In light of (B.1) and (10),  $(\partial(u_i)_D/\partial x, [u_k], [\sigma_{3k}])$  are related by three equations of general form (compare (12a)):

$$\sum_j C_j \frac{\partial}{\partial x} \int_{GX} d\xi f_j \int \frac{|p|}{p} dp \left( \frac{x_3}{|x_3|}, \frac{\sqrt{-p}}{\sqrt{p}} \right) \exp[p(x - \xi) - A\sqrt{-p}\sqrt{p}|x_3|] = 0. \quad (28)$$

The integration range for  $f_j = \partial(u_i)_D/\partial x$  is  $|\xi - r_S| < r_B$ , for  $f_j = [u_k]$  is  $r_+ < \xi < r_S$  and for  $f_j = [\sigma_{3k}]$  is  $-r_- < \xi < r_+$ . Three similar equations in terms of  $\partial(u_i)_S$ , with  $A$  replaced by  $B$ , follow from (B.2). Integration with respect to  $p$  [Brock 2015a; 2015b] and use of (10) give expressions  $\partial u_k/\partial x$  that are valid for  $(|x_3| \approx 0, x \rightarrow r_S^-)$ . The results for  $x_3 \approx 0(+)$  are given in Appendix C by (C.1)–(C.3). Expressions for  $\partial_1[u_3](|x_3| \approx 0, x \rightarrow r_S^-)$  can then be developed in a manner similar to that involving  $\partial_1 u_k$ . The last term in (23) entails integration over the tube with radius  $r_B \rightarrow 0$ . A standard polar coordinate system  $(r, \phi)$ , centered on  $B_C$ , is therefore defined for given  $\psi$  in the  $xx_3$ -plane by

$$r = \sqrt{(x - r_S)^2 + x_3^2}, \quad \phi = \tan^{-1} \frac{x_3}{x - r_S} \quad (|\phi| < \pi). \quad (29)$$

Combining (24b), (24c), (26) and (29) with the formulas based on (C.1)–(C.3) and corresponding formulas for  $x_3 \leq 0$  results in (C.4). Use of Green's theorem [Malvern 1969] in the dynamic steady state with translating basis  $\mathbf{x}$  produce for the last term in (23) an integral over the tube surface. Use of (C.4) and (C.5) then gives for this term

$$-\mu V \int_{\Psi} d\psi r_S \sqrt{D_S^2 + D_C^2} \left( \frac{\bar{c}^3 A}{\pi S} G_C D_S \right)^2 \int_{\Phi} E \cos \phi d\phi, \quad (30a)$$

with

$$E = \left( \frac{TA_+}{2AA_{\Phi}} + \frac{BB_+}{B_{\Phi}} \right)^2 + \left( \frac{TA_-}{2A_{\Phi}} + \frac{B_-}{B_{\Phi}} \right)^2. \quad (30b)$$

Symbol  $\Phi$  signifies integration over range  $|\phi| < \pi$ . Parameter  $\bar{c} \leq c < c_R < 1$ . Therefore, for speeds  $V$  which are rapid but well below Rayleigh value  $V_R = c_R V_S$ , first order expansions for  $(A, B)$  in (11c)

and  $(A_\Phi, B_\Phi)$  in (C.5) allow approximations

$$E = 2\bar{c}^4 \sin^2 \frac{\phi}{2} \left[ \frac{1}{c_D^4} + 4 \left( 1 - \frac{1}{c_D^2} \right)^2 \sin^4 \frac{\phi}{2} \cos^2 \phi \right] + O(\bar{c}^6), \quad (31a)$$

$$\int_\Phi E \cos \phi \, d\phi = -\pi c_1^4 E_\Phi, \quad E_\Phi = \frac{1}{4} \left[ \frac{1}{c_D^4} + \frac{23}{8} \left( 1 - \frac{1}{c_D^2} \right)^2 \right]. \quad (31b)$$

Equations (24), (27) and (30a) all involve integration with respect to  $\psi$  and exhibit speed  $V$  as factor, so that (23), (24a), (27b), (30a) and (31) give

$$\cos \psi \sqrt{D_S^2 + D_C^2} - P_C G_C^2 M D_S = 0, \quad (32a)$$

$$P_C = \frac{\mu}{\pi e_G} \frac{R}{2S}, \quad M = 1 + 2 \frac{(\bar{c}^2 A)^2}{SR} \bar{c}^2 E_\Phi D_S \sqrt{D_S^2 + D_C^2}. \quad (32b)$$

For  $|\psi| < \pi/2$ , (32a) and (24c) define a nonlinear differential equation for  $r_S(\psi)$ , but parameters  $r_C^-(\psi)$  and  $r_\pm(\psi)$  are also involved. Equation (18c) and continuity requirements  $r_+(\pm\pi/2) = r_-(\mp\pi/2)$  also serve as constraints upon (32a).

### Comment on effects of kinetic energy

In the limit as  $\bar{c} \rightarrow 0$

$$\frac{\bar{c}^2 A}{S} \rightarrow 1, \quad 2 \frac{\bar{c}^2 A}{R} \rightarrow \frac{c_D^2}{c_D^2 - 1}. \quad (33)$$

Thus the effect of kinetic energy ( $E_\Phi$ ) in (32a) is proportional to  $\bar{c}^2$ , i.e.,  $V^2$ . The term  $M$  is a magnification factor for this effect. Setting  $M = 1$  in (32a) leads for  $|\psi| < \pi/2$  to

$$D_S - \frac{D_C \cos \psi}{\sqrt{P_G^2 - \cos^2 \psi}} = 0 \quad (P_G = P_C G_C^2 > \cos \psi). \quad (34)$$

### Particular case: disk-shaped die

Consider the die to be a disk in the shape of ellipsoid of revolution

$$x_1^2 + x_2^2 + C_3 x_3^2 = r_0^2,$$

where  $(C_3 \gg 1)$ . Length  $r_0$  is the disk radius, and there should be clearance between disk edge and  $(B_S, B_C^-)$ . Moreover span  $l_C$  of  $A_C$  is assumed to be small. Thus for  $|\psi| < \pi/2$

$$l_C = r_+ + r_- \ll 2r_0, \quad (r_S, r_C^-) > r_0. \quad (35a)$$

In view of (4c) and (10)

$$\frac{\partial U}{\partial x} = -\frac{x}{\sqrt{C_3} r_0}. \quad (35b)$$

If the expectation that  $(r_S, r_C^-) \gg r_{\pm}$  is now also imposed, series expansions for functions of  $(r_S, r_C^-, r_{\pm})$  can be introduced. In particular integration in (18d) and (26c) can be performed analytically, and constraint I and key parameter  $G_C$  have asymptotic forms

$$r_+ + \Omega l_C - 1/2r_S(1 + r_S/r_C^-)[(r_+ + \Omega l_C/2)(r_+ + \Omega l_C) + \frac{3}{2}\Omega l_C r_-] = 0, \tag{36a}$$

$$G_C = \sqrt{r_S/C_3} \sqrt{1 + r_S/r_C^-} \frac{\pi S}{c^2 A r_0} (D_0 I_0 + D_1 I_1 + D_2 I_2). \tag{36b}$$

The  $(D, I)$ -terms in (36b) are given in Appendix D. Letting  $(r_S, r_C^-) \rightarrow \infty$  for  $|\psi| < \pi/2$  in (36a) gives the result found for sliding on a half-space by an axially symmetric die [Brock 2012]:

$$r_+ = -\Omega l_C, \quad r_- = (1 + \Omega)l_C. \tag{37}$$

Use of (35b) and (36b) in (22) yield asymptotic results  $x^* + r_- + \Omega l_C = 0$  and

$$\sigma(x^*) = \sigma^* = -\frac{\mu R}{S\sqrt{C_3}} \frac{l_C(1 + \Omega)^{1+\Omega}}{r_0(-\Omega)^\Omega} \left[ 1 + \frac{1}{2r_S}(1 + r_S/r_C^-)(r_+ + \Omega l_C) \right]. \tag{38}$$

The right hand side of (38) is negative, in accordance with constraint II. Constraint III requires that (38) be invariant for  $|\psi| < \pi/2$ .

For the disk, the framework developed for study is now seen to consist of:

- (a) Properties of the disk  $(r_0, C_3, c)$ , disk-solid  $(\gamma)$  and solid, e.g.,  $(\mu, c_D, c_R, e_G)$ .
- (b) Values of  $c$  such that  $V$  is well below  $V_R$ , but not negligible.
- (c) For these inputs, formulas for parameters  $(r_{\pm}, r_S, r_C^-)$  are to be determined from (32)–(38), Appendix D and invariance of (38). As is noted at the outset, this paper considers frictionless sliding contact. This does not mean that friction is a negligible effect: parameter  $\Omega$  in (19a) plays a key role in solution formulas derived above, and calculations in Table 1 for various  $c$  and  $(\gamma, \psi)$  suggest that friction effects, while small, become noticeable as sliding/crack growth speed  $V$  increases. For purposes of illustrating the use of the framework, and to take advantage of the low-speed kinetic

$(\psi, \gamma) \downarrow c \rightarrow$	0.05	0.1	0.2	0.3
$(\psi, 0)$	-0.5	-0.5	-0.5	-0.5
$(0^\circ, 0.2)$	-0.48424	-0.48399	-0.48367	-0.48306
$(0^\circ, 0.4)$	-0.46855	-0.46807	-0.46742	-0.46621
$(30^\circ, 0.2)$	-0.48634	-0.48608	-0.48594	-0.48556
$(30^\circ, 0.4)$	-0.47274	-0.47221	-0.47194	-0.47118
$(45^\circ, 0.2)$	-0.48813	-0.48868	-0.48861	-0.4884
$(45^\circ, 0.4)$	-0.47629	-0.47739	-0.47725	-0.47682
$(60^\circ, 0.2)$	-0.49211	-0.49212	-0.49201	-0.49192
$(60^\circ, 0.4)$	-0.48422	-0.48424	-0.48403	-0.48385
$(90^\circ, \gamma)$	-0.5	-0.5	-0.5	-0.5

**Table 1.** Parameter  $\Omega$  for various  $c$  and  $(\psi, \gamma)$ .

energy parameter result (31b) however, calculations for the disk are now presented for the case  $\Omega = -0.5$  ( $\gamma = 0$ ).

### Crack/contact zone contours: key equations

The algebraic manipulations involved in studying the geometry of crack and contact zone contours with the formulas derived thus far are simpler if performed, in part, in terms of parameters

$$l_C = r_+ + r_-, \quad d_C = r_+ - r_-, \quad \beta = r_S/r_C^-. \quad (39)$$

Equations (36a) and (38) now give for  $|\psi| < \pi/2$ ,

$$\frac{l_C}{r_0} = \chi/3[1 + 2\beta - (1 + \beta/2)\sqrt{1 + \beta}\sqrt{(\chi r_0)/(6r_S)}], \quad (40a)$$

$$\frac{d_C}{r_0} = -\frac{3}{16}(\chi/3)^2(1 + \beta)(1 + 2\beta)^2 r_0/r_S, \quad (40b)$$

$$\chi = \frac{2\bar{c}^2 A}{\mu R} \sqrt{C_3} |\sigma^*| (\chi, r_0/r_S) < 1. \quad (40c)$$

In appropriate fashion  $(l_C, d_C, r_{\pm}) = 0$  when  $|\sigma^*| = 0$  ( $\chi = 0$ ). The quantity  $d_C = 0$  when  $r_S \rightarrow \infty$ , a result consistent with (37) when  $\gamma = 0$ . Use of (36a), (39) and (40) in (32) when  $\gamma = 0$  gives for  $|\psi| < \pi/2$ :

$$\cos \psi \sqrt{D_S^2 + D_C^2} - P M r_0/r_S D_S = 0. \quad (41)$$

In (41) we have

$$M = 1 + \frac{2\bar{c}^4 A}{R} E_\Phi D_S \sqrt{D_S^2 + D_C^2}, \quad (42a)$$

$$P = \frac{\pi}{C_3} \frac{\mu r_0}{e_G} \frac{R}{2\bar{c}^2 A} (\chi/4)^4 F(\beta) \left( P \frac{r_0}{r_S} > \cos \psi \right), \quad (42b)$$

$$F(\beta) = \left(\frac{2}{3}\beta\right)^2 (1 + \beta)(1 + 2\beta)^4. \quad (42c)$$

For  $\psi = 0$  (41) and (42) give

$$\frac{r_S}{r_0} = P_1 M_1, \quad \frac{r_C^-}{r_0} = \frac{r_S}{\beta_1 r_0} \left( \frac{r_S}{r_0}, \frac{r_C^-}{r_0} \right) > 1, \quad (43a)$$

$$M_1 = 1 + \frac{2c^4 A_1}{E_\Phi}, \quad (43b)$$

$$P_1 = \frac{\pi}{C_3} \frac{\mu r_0}{e_G} \frac{R_1}{2c^2 A_1} (\chi_1/4)^4 F(\beta_1), \quad \chi_1 = \frac{2c^2 A_1}{\mu R_1} \sqrt{C_3} |\sigma^*| < 1. \quad (43c)$$

Subscript 1 signifies that  $\bar{c} \rightarrow c$  in (11a) and (11b).

For  $|\psi| \rightarrow \pi/2$ ,

$$r_S \approx \frac{h_S}{\cos \psi}, \quad r_C^- \approx \frac{h_C^-}{\cos \psi}, \tag{44a}$$

$$\frac{h_S}{r_0} = P_2 M_2, \quad \frac{h_C^-}{r_0} = \frac{h_S}{\beta_2 r_0}, \tag{44b}$$

$$M_2 = 1 + \frac{c_D^2 c^2}{c_D^2 - 1} E_\Phi, \tag{44c}$$

$$P_2 = \frac{\pi}{C_3} \frac{\mu r_0}{e_G} (1 - 1/c_D^2)^3 \left( \frac{\sqrt{C_3}}{4\mu} |\sigma^*| \right)^4 F(\beta_2). \tag{44d}$$

Subscript 2 signifies that  $\bar{c} \rightarrow 0$  in (11).

Equations (10) and (44) show that points on  $(B_S, B_C^-)$  approach rectilinear asymptotes that parallel the  $x_2$ -axis at great distances from the path of the die. That is,

$$B_S : x_1 \rightarrow h_C, \quad |x_2| \rightarrow \infty, \tag{45a}$$

$$B_C^- : x_1 \rightarrow -h_C^-, \quad |x_2| \rightarrow \infty. \tag{45b}$$

Term  $M$  in (32) and (42a) is the magnification factor for the effect of kinetic energy, and  $(M_1, M_2)$  are limit cases. To illustrate their behavior, consider a generic solid with properties [Brock and Georgiadis 2000; deBoer et al. 1988; Skriver and Rosengaard 1992]:

$$\begin{aligned} \mu &= 79 \text{ GPa}, & |\sigma_Y| &= 250 \text{ MPa}, & e_G &= 2.2 \text{ J/m}^2 \\ V_S &= 3094 \text{ m/s}, & c_D &= 2.0, & c_R &= 0.933. \end{aligned}$$

Here  $|\sigma_Y|$  is the magnitude of the yield stress in compression. Calculations of (43b) and (44c), based on these properties, are given in Table 2 for various values of  $c$ . Entries show that the kinetic energy effect in  $M_1$  and  $M_2$  reaches 17% and 14%, respectively, when  $V = 0.536V_R$ . In view of (31) therefore, subsequent calculations are restricted to range  $0 < c < 0.5$ .

**Crack/contact zone contours: calculations**

Table 2 indicates that kinetic energy is a perturbation in the study of crack and contact zone contours for  $\psi = 0$  and  $|\psi| \rightarrow \pi/2$ . Equation (34) and rearrangement of (32a) however show that kinetic energy serves as a singular perturbation in the governing differential equation for  $0 < |\psi| < \pi/2$ ,

$$D_C^2 + \left[ \left( \frac{r_S}{r_0 P} \cos \psi - \frac{2\bar{c}^4 A}{R} E_\Phi D_S^2 \right)^2 - 1 \right] D_S^2 = 0. \tag{46a}$$

$c$	0.05	0.1	0.2	0.5
$M_1$	1.00139	1.00563	1.02304	1.1734
$M_2$	1.0014	1.0056	1.0224	1.1394

**Table 2.** Parameters  $(M_1, M_2)$  for various  $c$ .

$c$	0.05	0.1	0.2	0.4	0.5
$C_3^*$	$5.67(10^4)$	$5.56(10^4)$	$5.34(10^4)$	$4.36(10^4)$	$3.65(10^4)$

**Table 3.**  $C_3^*$  ( $\chi_1 = 1, |\sigma^*| = |\sigma_Y|$ ).

Study of (46a) near  $\psi \approx 0$  for a given ratio  $\beta = r_S/r_C^-$  suggests asymptotic solution

$$\frac{r_S}{r_0} \approx \frac{\mu r_0}{C_3 e_G} \frac{\pi F(\beta_1)}{\cos \psi} \left( \frac{\chi_1}{4} \right)^4 \left( \frac{R_1}{2c^2 A_1} + c^2 E_\Phi \right). \quad (46b)$$

This result agrees with (43) at  $\psi = 0$  and approximates the asymptotic behavior of (43a) for  $|\psi| \rightarrow \pi/2$ . In view of (10) therefore asymptotic formulas for contours ( $B_S, B_C^-$ ) are, respectively

$$\sqrt{x_1^2 + x_2^2} \approx r_S \quad (x_1 > 0), \quad \sqrt{x_1^2 + x_2^2} \approx r_C^- \quad (x_1 < 0). \quad (46c)$$

Equations (44a) and (46c) suggest a results similar to that described in [Brock 2015b]. The crack gap lies in a band which bulges outward from the die along its path, but forms a strip of finite width far away from the path.

Results (43)–(45) and related calculations for  $\psi = 0$  and  $|\psi| \rightarrow \pi/2$  by themselves allow insight into contour geometry. Parameter  $\sigma^*$  is the maximum compressive stress in contact zone  $A_C$  formed by the disk, and for the ellipsoidal disk,  $1/\sqrt{C_3}$  is the disk thickness-diameter ratio. These are coupled in  $(\chi, \chi_1)$ , where  $\chi_1 > \chi$  ( $0 < |\psi| < \pi/2$ ). Analysis is elastic, so  $|\sigma^*| < |\sigma_Y|$ , and approximation (40) requires that  $\chi < 1$ . Limit case ( $\chi_1 = 1, |\sigma^*| = |\sigma_Y|$ ) examination shows that constraint  $C_3 < C_3^*$  applies. Calculations of  $C_3^*$  for the generic solid in Table 3 imply that the disk can be essentially flat. These observations suggest examining parameters ( $l_C, d_C$ ) for contact zone  $A_C$ , and  $(\beta_1, \beta_2)$  for crack gap  $A_G$ .

For the same generic solid we choose subcritical values  $|\sigma^*| = 150$  MPa and  $C_3 = 10000$ , with disk radius  $r_0 = 0.05$  m and clearance ratios

$$\frac{r_S}{r_0} = 4 \quad (\psi = 0), \quad \frac{h_S}{r_0} = 1 \quad (|\psi| \rightarrow \pi/2).$$

In Tables 4 and 5 values of, respectively,  $l_C/r_0$  and  $d_C/r_0$ , for  $\psi = 0$  are given for various  $(c, \beta_1)$ . Corresponding values  $\beta_2$  follow from (43a) and (44b) as roots of

$$F(\beta_2) - \frac{M_1}{M_2} \left[ \frac{2c^2 A_1}{R_1} \left( 1 - \frac{1}{c_D^2} \right) \right]^3 F(\beta_1) = 0. \quad (47)$$

$c \downarrow \beta_1 \rightarrow$	0.01	0.1	0.2	0.5	0.8
0.05	0.075	0.091	0.107	0.154	0.201
0.1	0.077	0.092	0.108	0.155	0.203
0.2	0.82	0.096	0.114	0.165	0.215
0.5	0.094	0.112	0.115	0.19	0.248

**Table 4.**  $l_C/r_0$  ( $r_S/r_0 = 4, \psi = 0$ ).



$c \downarrow \beta_1 \rightarrow$	0.01	0.1	0.2	0.5	0.8
0.05	-0.0034	-0.00052	-0.00077	-0.00194	-0.004
0.1	-0.00035	-0.00053	-0.00077	-0.002	-0.004
0.2	-0.0004	-0.0006	-0.00088	-0.0022	-0.0046
0.5	-0.00053	-0.00081	-0.0012	-0.003	-0.0062

**Table 5.**  $d_C/r_0$  ( $r_S/r_0 = 4, \psi = 0$ ).

$\beta_1$	0.01	0.1	0.2	0.5	0.8	1.0
$\beta_2$	0.00271	0.0564	0.117	0.275	0.55	0.825
$l_C/r_0$	0.0756	0.084	0.093	0.118	0.16	0.205

**Table 6.** Values of  $(\beta_1, \beta_2, l_C/r_0)$  for  $r_S/r_0 = 4, h_S/r_0 = 2$  and  $c = 0.2$ .

Study of (42c) for  $\beta > 0$  shows that  $F > 0$ , with rapid monotonic growth. Thus numerical determination of roots is not difficult. Based on (47) therefore, a snapshot of how gap-die clearance ratios  $(\beta_1, \beta_2)$  compare is given in Table 6. Corresponding values of  $l_C/r_0$  ( $|\psi| \rightarrow \pi/2$ ) are also given ( $d_C = 0$ ).

**Some observations**

This paper considered crack growth in the dynamic steady state caused by the translation of a rigid, smooth die between the surfaces of an initially closed slit. Analysis produced a nonlinear differential equation for the radial distance  $r_S(\psi)$  from the die center to the crack edge, where  $\psi$  is the angle with respect to the path of die translation. Equation coefficients, however, depend on radial distances  $r_{\pm}(\psi)$  and  $r_C^-(\psi)$  to the contours of respectively the crack/die contact zone and the closure zone, i.e., the region in the wake of the die where crack surfaces resume contact. Moreover, the sliding contact aspects of the process lead to algebraic constraints. A framework of equations for the process is thus generated, and was studied to gain insight into the geometry of crack and contact zone behavior. In addition to various formulas:

- (a) Calculations in Table 1 show that neglect of sliding friction could affect solution behavior as die/crack growth speed increases.
- (b) Calculations in Table 2 show that inclusion of kinetic energy is a perturbation for significant, but clearly subcritical, die/crack growth speeds.
- (c) Calculations in Table 3 illustrate the relationship between thickness of a disk-shaped die and maximum allowable die/crack contact zone compression.
- (d) Calculations in Tables 4 and 5 show that contact zone width and location of its center with respect to die center are sensitive to die/crack growth speed. They are also sensitive to the relative distances, measured along the die path, from die center to crack edge and crack closure contour. For example, consider in Table 4 the die speed that is 20% of the shear speed in the solid: if the closure contour is 100 times further away from the die center than is the crack edge, contact zone width is 8.2% of the die radius. If it is only 1.25 times further away, the ratio is 24.9%.

- (e) Calculations in Tables 4–6 show that the relative distances measured along the die path are greater than relative distances far away from the die path. This observation, together with formulas, show that the gap opened up by die-induced fracture is an infinitely long slit of finite width; its contours bulge out from the die near its path, but are rectilinear and parallel far away.

Die sliding was frictionless, but friction was considered in derivation of the framework. A complete solution for the nonlinear differential equation was not attempted. Thus, The framework was not fully utilized here. However, general conclusions concerning the geometry of crack and contact zones did emerge. These conclusions and the equations themselves could provide the basis for a more general investigation.

### Appendix A

$$U_D^{(\pm)} = \frac{-1}{2c_1^2 A} \left[ T[\hat{u}_3] + \frac{1}{\mu} (p_1[\hat{\sigma}_{31}] + p_2[\hat{\sigma}_{32}]) \right] (\pm) \frac{1}{c_1^2} \left( p_1[\hat{u}_1] + p_2[\hat{u}_2] + \frac{[\hat{\sigma}_{33}]}{2\mu} \right), \quad (\text{A.1a})$$

$$V_1^{(\pm)} = \frac{p_1 B}{c_1^2} [\hat{u}_3] + \frac{1}{2\mu B c_1^2} [p_1 p_2 [\hat{\sigma}_{32}] - (p_2^2 + B^2) [\hat{\sigma}_{31}]] (\pm) \frac{1}{2} \left( [\hat{u}_1] - \frac{p_1 [\hat{\sigma}_{33}]}{\mu c_1^2} \right) \\ \mp \frac{p_1}{c_1^2} (p_1 [\hat{u}_1] + p_2 [\hat{u}_2]), \quad (\text{A.1b})$$

$$V_2^{(\pm)} = \frac{p_2 B}{c_1^2} [\hat{u}_3] + \frac{1}{2\mu B c_1^2} [p_1 p_2 [\hat{\sigma}_{31}] - (p_1^2 + B^2) [\hat{\sigma}_{32}]] (\pm) \frac{1}{2} \left( [\hat{u}_2] - \frac{p_2 [\hat{\sigma}_{33}]}{\mu c_1^2} \right) \\ \mp \frac{p_2}{c_1^2} (p_1 [\hat{u}_1] + p_2 [\hat{u}_2]). \quad (\text{A.1c})$$

Equation (8c) holds for (A.1), and it is noted that  $p_1 \hat{V}_1^{(\pm)} + p_2 \hat{V}_2^{(\pm)}$  gives

$$\frac{B}{c_1^2} \left[ (p_1^2 + p_2^2) [\hat{u}_3] - \frac{1}{2\mu} (p_1 [\hat{\sigma}_{31}] + p_2 [\hat{\sigma}_{32}]) \right] (\pm) \frac{1}{2c_1^2} \left[ T(p_1 [\hat{u}_1] + p_2 [\hat{u}_2]) - B(p_1^2 + p_2^2) \frac{[\hat{\sigma}_{33}]}{\mu} \right]. \quad (\text{A.2})$$

For  $x_3 = 0(+)$  use of (A.1) and (A.2) lead to

$$[\hat{u}_1] - \frac{1}{\mu D_R B} (p_2^2 D_M - c_1^2 B^2) \left( 2\hat{\sigma}_{31}^{(+)} - [\hat{\sigma}_{31}] - \frac{D_N}{c_1^2 B} p_1 [\hat{\sigma}_{33}] \right) \\ + p_1 p_2 \frac{D_M}{\mu D_R B} \left( 2\hat{\sigma}_{32}^{(+)} - [\hat{\sigma}_{32}] - \frac{D_N}{c_1^2 B} p_2 [\hat{\sigma}_{33}] \right) = 0, \quad (\text{A.3a})$$

$$[\hat{u}_2] - \frac{1}{\mu D_R B} (p_1^2 D_M - c_1^2 B^2) \left( 2\hat{\sigma}_{32}^{(+)} - [\hat{\sigma}_{32}] - \frac{D_N}{c_1^2 B} p_2 [\hat{\sigma}_{33}] \right) \\ + p_1 p_2 \frac{D_M}{\mu D_R B} \left( 2\hat{\sigma}_{31}^{(+)} - [\hat{\sigma}_{31}] - \frac{D_N}{c_1^2 B} p_1 [\hat{\sigma}_{33}] \right) = 0, \quad (\text{A.3b})$$

$$[\hat{u}_3] - \frac{c_1^2 A}{\mu D_R} \left[ 2\hat{\sigma}_{33}^{(+)} - [\hat{\sigma}_{33}] - \frac{D_N}{c_1^2 B} (p_1 [\hat{\sigma}_{32}] + p_2 [\hat{\sigma}_{31}]) \right] = 0. \quad (\text{A.3c})$$

Terms ( $D_R$ ,  $D_N$ ,  $D_M$ ) in (A.3) are given by

$$D_R = T^2 + 4(p_1^2 + p_2^2)AB, \quad D_N = T - 2AB, \quad D_M = 2D_N + c_1^2, \quad (\text{A.4a})$$

$$T = (c^2 - 2)p_1^2 - 2p_2^2. \quad (\text{A.4b})$$

### Appendix B

In view of (15)–(17), Equations (A.1) and (7) give for  $x_3 > 0(-)$  and  $x_3 < 0(+)$ ,

$$(\hat{u}_1)_D + \frac{p_1}{2c_1^2 A} (T[\hat{u}_3] + p_1[\hat{\sigma}_{31}]/\mu) \exp(-A|x_3|) = 0, \quad (\text{B.1a})$$

$$(\hat{u}_2)_D + \frac{p_2}{2c_1^2 A} (T[\hat{u}_3] + p_1[\hat{\sigma}_{31}]/\mu) \exp(-A|x_3|) = 0, \quad (\text{B.1b})$$

$$(\hat{u}_3)_D(\mp) \frac{1}{2c_1^2} (T[\hat{u}_3] + p_1[\hat{\sigma}_{31}]/\mu) \exp(-A|x_3|) = 0. \quad (\text{B.1c})$$

$$(\hat{u}_1)_S - \frac{1}{c_1^2} \left[ p_1 B[\hat{u}_3] - \frac{1}{2B} (p_2^2 + B^2)[\hat{\sigma}_{31}]/\mu \right] \exp(-B|x_3|) = 0, \quad (\text{B.2a})$$

$$(\hat{u}_2)_S - \frac{1}{c_1^2} \left( p_2 B[\hat{u}_3] - \frac{p_1 p_2}{2B} [\hat{\sigma}_{31}]/\mu \right) \exp(-B|x_3|) = 0, \quad (\text{B.2b})$$

$$(\hat{u}_3)_S(\mp) \frac{1}{c_1^2} \left[ (p_1^2 + p_2^2)[\hat{u}_3] - \frac{p_1}{2} [\hat{\sigma}_{31}] \right] \exp(-B|x_3|) = 0. \quad (\text{B.2c})$$

### Appendix C

$$\frac{\partial u_1^{(+)}}{\partial x} \approx -\frac{A \cos \psi}{\pi^2 S} \int_C \frac{\partial U}{\partial t} \sqrt{\frac{r_S - t}{t + r_C^-}} \frac{(t + r_-)^\Omega dt}{(r_+ - t)^{1+\Omega}} \text{Re} Q_+(i2P_{12}, t), \quad (\text{C.1a})$$

$$\frac{\partial u_2^{(+)}}{\partial x} \approx -\frac{A \sin \psi}{\pi^2 S} \int_C \frac{\partial U}{\partial t} \sqrt{\frac{r_S - t}{t + r_C^-}} \frac{(t + r_-)^\Omega dt}{(r_+ - t)^{1+\Omega}} \text{Re} Q_+(i2P_{12}, t), \quad (\text{C.1b})$$

$$\frac{\partial u_3^{(+)}}{\partial x} \approx \frac{A}{\pi^2 S} \int_C \frac{\partial U}{\partial t} \sqrt{\frac{r_S - t}{t + r_C^-}} \frac{(t + r_-)^\Omega dt}{(r_+ - t)^{1+\Omega}} \text{Im} Q_+(i2P_3, t). \quad (\text{C.1c})$$

$$Q_+(f, t) = \int_+ \sqrt{\frac{\tau + r_C^-}{r_S - \tau}} \frac{f(\tau - r_+)^{1+\Omega}}{(\tau + r_-)^\Omega (t - \tau)} d\tau. \quad (\text{C.2})$$

In (C.2) integration subscript + signifies range  $r_+ < \tau < r_S$ , and in (C.1)

$$P_{12} = \frac{T}{2A(z_A - \tau)} + \frac{B}{z_B - \tau}, \quad P_3 = \frac{T}{2(z_A - \tau)} + \frac{1}{z_B - \tau}, \quad (\text{C.3a})$$

$$z_A = x + iA|x_3|, \quad z_B = x + iB|x_3|. \quad (\text{C.3b})$$

In light of (24a), (24c), (26c) and (29) results for  $r \rightarrow 0$ ,  $|\phi| < \pi$ ,  $|\psi| < \pi/2$  are

$$\partial_1 u_1 \rightarrow -\frac{\cos \psi}{\sqrt{2r}} \frac{2A}{\pi S} G_C D_S \left( \frac{T}{2A} \frac{A_+}{A_\Phi} + B \frac{B_+}{B_\Phi} \right) \text{sgn}(\phi), \quad (\text{C.4a})$$

$$\partial_1 u_2 \rightarrow -\frac{\sin \psi}{\sqrt{2r}} \frac{2A}{\pi S} G_C D_S \left( \frac{T}{2A} \frac{A_+}{A_\Phi} + B \frac{B_+}{B_\Phi} \right) \text{sgn}(\phi), \quad (\text{C.4b})$$

$$\partial_1 u_3 \rightarrow -\frac{1}{\sqrt{2r}} \frac{2A}{\pi S} G_C D_S \left( \frac{T}{2} \frac{A_-}{A_\Phi} + \frac{B_-}{B_\Phi} \right). \quad (\text{C.4c})$$

$$A_\Phi = \sqrt{1 - \bar{c}^2 / c_D^2 \sin^2 \phi}, \quad A_\pm = \sqrt{A_\Phi \pm \cos \phi}, \quad (\text{C.5a})$$

$$B_\Phi = \sqrt{1 - \bar{c}^2 \sin^2 \phi}, \quad B_\pm = \sqrt{B_\Phi \pm \cos \phi}. \quad (\text{C.5b})$$

### Appendix D

$$D_0 = 1 - 1/r_S(r_+ + \Omega l_C) + \Omega(1 + \Omega)(l_C/(2r_S))^2, \quad (\text{D.1a})$$

$$D_1 = 1/(2r_S)(r_S/r_C^- - 1)[1 - 2/r_S(r_+ + \Omega l_C)], \quad (\text{D.1b})$$

$$D_2 = 1/(2r_S^2) \left[ \frac{3}{4}(r_S/r_C^- - 1)^2 + r_S/r_C^- \right]. \quad (\text{D.1c})$$

$$I_0 = r_+ + \Omega l_C, \quad (\text{D.2a})$$

$$I_1 = r_+^2 + \Omega r_+ l_C - \Omega/2(1 - \Omega)l_C^2, \quad (\text{D.2b})$$

$$I_2 = r_+^3 + 3\Omega r_+^2 l_C - 3\Omega/2(1 - \Omega)r_+ l_C^2 + \Omega/6(1 - \Omega)(2 - \Omega)l_C^3. \quad (\text{D.2c})$$

### References

- [Brock 2004] L. M. Brock, "Dynamic fracture of transversely isotropic coupled thermoelastic solids: wedging by a cylinder with friction", *J. Therm. Stresses* **27**:11 (2004), 1053–1073.
- [Brock 2012] L. M. Brock, "Two cases of rapid contact on an elastic half-space: the sliding ellipsoid die, rolling sphere", *J. Mech. Mater. Struct.* **7**:5 (2012), 469–483.
- [Brock 2015a] L. M. Brock, "Contours for planar cracks growing in three dimensions", *J. Mech. Mater. Struct.* **10**:1 (2015), 63–77.
- [Brock 2015b] L. M. Brock, "Contours for planar cracks growing in three dimensions: influence of kinetic energy", *J. Appl. Mech. (ASME)* **82**:11 (09/28 2015), 111011.
- [Brock and Georgiadis 2000] L. M. Brock and H. G. Georgiadis, "Sliding contact with friction of a thermoelastic solid at subsonic, transonic, and supersonic speeds", *J. Therm. Stresses* **23**:7 (2000), 629–656.
- [deBoer et al. 1988] F. R. deBoer, R. Boom, W. C. M. Mattens, A. R. Miedema, and A. K. Niessen, *Cohesion in metals*, North-Holland, Amsterdam, 1988.
- [Freund 1972] L. B. Freund, "Energy flux into the tip of an extending crack in an elastic solid", *J. Elasticity* **2**:4 (1972), 341–349.
- [Freund 1990] L. B. Freund, *Dynamic fracture mechanics*, Cambridge Monographs on Mechanics and Applied Mathematics, Cambridge University Press, Cambridge, England, 1990.

- [Gdoutos 2005] E. E. Gdoutos, *Dynamic fracture*, pp. 239–264, Solid mechanics and its applications **123**, Springer, New York, 2005.
- [Malvern 1969] L. S. Malvern, *Introduction to the mechanics of continuous media*, Prentice-Hall, Englewood Cliffs, New Jersey, 1969.
- [Mastrojannis et al. 1980] E. N. Mastrojannis, L. M. Keer, and T. Mura, “Growth of planar cracks induced by hydraulic fracturing”, *Int. J. Numer. Meth. Eng.* **15**:1 (1980), 41–54.
- [Skriver and Rosengaard 1992] H. L. Skriver and N. M. Rosengaard, “Surface energy and work function of elemental metals”, *Phys. Rev. B* **46** (Sep 1992), 7157–7168.
- [Sneddon 1972] I. N. Sneddon, *The use of integral transforms*, McGraw-Hill, New York, 1972.

Received 25 Feb 2016. Revised 4 Apr 2016. Accepted 6 Aug 2016.

LOUIS M. BROCK: [louis.brock@uky.edu](mailto:louis.brock@uky.edu)

*Department of Mechanical Engineering, College of Engineering, University of Kentucky, Lexington, KY 40506-0038, United States*



# JOURNAL OF MECHANICS OF MATERIALS AND STRUCTURES

[msp.org/jomms](http://msp.org/jomms)

Founded by Charles R. Steele and Marie-Louise Steele

## EDITORIAL BOARD

ADAIR R. AGUIAR	University of São Paulo at São Carlos, Brazil
KATIA BERTOLDI	Harvard University, USA
DAVIDE BIGONI	University of Trento, Italy
YIBIN FU	Keele University, UK
IWONA JASIUK	University of Illinois at Urbana-Champaign, USA
C. W. LIM	City University of Hong Kong
THOMAS J. PENCE	Michigan State University, USA
GIANNI ROYER-CARFAGNI	Università degli studi di Parma, Italy
DAVID STEIGMANN	University of California at Berkeley, USA
PAUL STEINMANN	Friedrich-Alexander-Universität Erlangen-Nürnberg, Germany

## ADVISORY BOARD

J. P. CARTER	University of Sydney, Australia
D. H. HODGES	Georgia Institute of Technology, USA
J. HUTCHINSON	Harvard University, USA
D. PAMPLONA	Universidade Católica do Rio de Janeiro, Brazil
M. B. RUBIN	Technion, Haifa, Israel

**PRODUCTION** [production@msp.org](mailto:production@msp.org)

SILVIO LEVY Scientific Editor

Cover photo: Mando Gomez, [www.mandolux.com](http://www.mandolux.com)

---

See [msp.org/jomms](http://msp.org/jomms) for submission guidelines.


---

JoMMS (ISSN 1559-3959) at Mathematical Sciences Publishers, 798 Evans Hall #6840, c/o University of California, Berkeley, CA 94720-3840, is published in 10 issues a year. The subscription price for 2017 is US \$615/year for the electronic version, and \$775/year (+\$60, if shipping outside the US) for print and electronic. Subscriptions, requests for back issues, and changes of address should be sent to MSP.

---

JoMMS peer-review and production is managed by EditFlow<sup>®</sup> from Mathematical Sciences Publishers.

PUBLISHED BY

 **mathematical sciences publishers**  
nonprofit scientific publishing

<http://msp.org/>

© 2017 Mathematical Sciences Publishers

# Journal of Mechanics of Materials and Structures

Volume 12, No. 2

March 2017

---

- A note on cross product between two symmetric second-order tensors**  
LÁSZLÓ SZABÓ 147
- Fracture in three dimensions due to die motion on crack surfaces: framework for study of crack/contact zone geometry**  
LOUIS M. BROCK 159
- Maxwell's equivalent inhomogeneity and remarkable properties of harmonic problems involving symmetric domains**  
SOFIA G. MOGILEVSKAYA and DMITRY NIKOLSKIY 179
- Interfacial microscopic boundary conditions associated with backstress-based higher-order gradient crystal plasticity theory**  
MITSUTOSHI KURODA 193
- Conjugate stress/strain base pairs for planar analysis of biological tissues**  
ALAN D. FREED, VEYSEL EREL and MICHAEL R. MORENO 219